Journal of Mathematical Chemistry Vol. 33, Nos. 3–4, May 2003 (© 2003)

Lattice structure of phospholipidic molecular domains at the liquid–gas interface

Adel F. Antippa

Département de Physique, Université du Québec à Trois-Rivières, 3351 Boul. des Forges, Trois-Rivières, Québec, Canada G9A 5H7
E-mail: antippa@mailaps.org

Received 25 November 2002

We make a mathematical analysis of the structure of the two dimensional lattice formed by the centers of parallely aligned and arbitrarily oriented spherocylindrical phospholipidic molecules hexagonally packed in cylindrical domains forming a monomolecular Langmuir film at the liquid–gas interface. The analysis is carried out as a function of the tilting angle θ and the tilting azimuth ϕ. We give a number of expressions for the *lattice radius vector*, and introduce the *Lattice Generating Operator*. We also present a number of theorems dealing with the existence and characteristics of the *common points of tangency*, the *double stationary points*, the *locus circles*, and the *envelop circles*, related to the lattice sites.

KEY WORDS: Langmuir, monolayer, domain, lattice, structure

1. Introduction

Overview

The present work is the fifth in a series of articles, [1–4] dealing with the detailed analytical modeling of Langmuir films as two dimensional conglomerates of phospholipidic domains of parallely aligned and arbitrarily oriented spherocylindrical molecules. The present article focuses on the structure of the two-dimensional lattice formed by the centers of the molecules. This lattice provides the infrastructure for the analytical description of domains. An understanding of its characteristics is crucial for the ability to simplify the mathematical expressions arising in the evaluation of the physical properties of the domain. The degree of simplification will, to a large extent, determine the possibility of successfully extending the detailed analytic description of domains to one further level of complexity, that is to systems, such as Langmuir films, that have domains as building blocks.

Relevance

Due to the considerable delocalization (smearing out) of atoms in molecules at biologically relevant probe energies (see Nagle and Tristram-Nagle [5]), as well as the in-

herent (quantum) delocalization of electrons in atoms, spherocylindrical (*rod-like*) molecules [6,7] provide a reasonably realistic [1], and analytically manageable [2,4], model for phospholipidic molecules. Furthermore, the existence of *domains* in Langmuir and Langmuir–Blodgett films, as well as in phospholipidic bilayers, is well established, and the importance of the role played by the collective *orientation* of the molecules in domains is well recognized (see the comprehensive discussions by McConnell [8], Ulman [9], Zasadzinski et al. [10,11], Katsaras [12], Knobler [13,14], Katsaras and Gutberlet [15]).

Literature

As experimental techniques become more sophoisticated, experimental investigations of amphiphilic monolayers, bilayers, and thin films at the air–water interface and on solid substrates are increasingly focalizing their attention on *domains*, *texture* and *orientational order* (both *tilt* and *azimuth*) at the molecular level. This trend is clearly visible in the intensive experimental studies of the last two decades, using a number of techniques like *X-ray diffraction* [16–27], *atomic force microscopy* [28–36], *scanning force microscopy* [37–40], *scanning tunneling microscopy* [41], *Brewester angle microscopy* [25–27,42–48], *fluorescence microscopy* [42,49–57], *liquid crystal optical amplification* [58], *neutron scattering* [59–61], and *lateral-force microscopy* [62]. The same trend towards a detailed study of *domains*, *texture* and *orientational order* at the molecular level is also visible in *phenomenological* [63,64], *simulation* [65,66], and *theoretical* [67–74] investigations.

Impact

Biological systems, are inherently multi-scale systems that cannot be adequately understood one scale at a time. Membrane gates, for example, open and close in reaction to the displacement of few ions. Thus in the long run, there is no viable biologically relevant theoretical alternative to the detailed multi-scale analysis which is characteristic of the present project, and the litterature review presented in previous section does support this point of view.

The results obtained here, as well as in [1–4], provide a useful starting point for perturbation calculations, for the determination of initial parameters in numerical simulations, for guiding experimental design, and for modeling related structural problems like mixed monolayers, fluctuating molecules, and imbedded proteins.

Results

The analytic expression for the lattice formed by the centers of parallely aligned and arbitrarily oriented spherocylindrical molecules was obtained in [3]. In the present work we will give several additional expressions for this lattice, leading to the introduction of the *Lattice Generating Operator*, which generates the whole lattice from a unite

vector along a secondary axis of symmetry. We also introduce the *phase angle* related to a lattice site.

As the tilting direction (tilt azimuth) ϕ varies, each lattice site describes a *locus*. We show that this locus is a circle. Furthermore, we show that the locus circles corresponding to different values of the tilting angle θ have a *common point of tangency*, and that this point of tangency coincides with the corresponding lattice site of the reference lattice. This common point of tangency is also the point nearest the origin on the locus circle, and lies on the radius vector from the origin to the center of the locus circle. We also show that the common point of tangency is a *double stationary point* of the projection (on the plane of the lattice) of the molecular axis. That is, all the projections (as a function of θ and ϕ) of the molecular axis intersect at this point. Finally, we show that this common point of tangency is the center of an *envelope circle* for the boundaries of the projection (on the plane of the lattice) of the cylindrical part of the molecule.

Outline

In section 2 we setup the problem by briefly recalling the essential features of the underlying model, the coordinate systems used, and the expression for the Tilting Operator. In section 3 we present several expressions for the lattice formed by the molecular centers. In section 4 we analyze these latter results in order to bring out the characteristics and symmetries of the lattice. In section 5 we present graphical simulations of the analytical results obtained in the two previous sections. These provide visual proofs of the validity of the analytical results. Appendix A is a compendium of needed results concerning the rotation operator and its applications. In appendix B, the expression for the lattice generating operator is worked out for the special case $\phi = 0$, as one more test of the validity of the analytical results.

2. The background

2.1. Model

The model used here is that of *spherocylindrical molecules* that are *parallely aligned*, *arbitrarily oriented*, and *closely packed* in *freely rotating cylindrical domains*. We will only give a brief summary of the essential features of the model, and refer the reader to [1–4], for details and justification. Globally the system we are dealing with is made up of phospholipidic molecules arranged in domains forming a Langmuir film at the liquid–gas interface. The molecules in a domain are aligned parallel to each other (see [2, figure 3]). Their collective orientation is given by the spherical angles θ and ϕ, (see [4, figure 1]) where the z-axis is in the direction of the normal to the interface. The molecules are assumed to be embedded in identical "virtual", rod-like [6], spherocylinders [7], having radius r_0 and cylindrical height h (see [2, figures 1, 2 and 7]). As the molecules are inclined they slide along each other (obliquely) in order for their polar heads to remain tangent to a plane parallel to the interface (see [3, figures 5–8]).

Each assembly of parallel molecules forms a "physical domain". When this assembly rotates freely about the normal to the interface, it occupies a cylindrical space which we refer to as the virtual domain, or simply the domain (see [4, figure 2]). Hence the domains of a Langmuir film are "virtual" right circular cylinders enveloping (circumscribing) the "physical domains" of the film. Their axes are perpendicular to the liquid–gas interface. Their radii R and heights H are determined by the condition that R and H, for each domain, be as small as possible. The height H, for each domain, is given by $H(r_0, h, \theta) = 2r_0 + h\cos\theta$, while the radius R of a domain is equal to half the largest dimension of the projection of the "physical domain" on the interface. The plane perpendicular to the symmetry axis of the domain and situated halfway in-between its base and top is the halfway plane (see [4, figure 3]). The cross section of the domain in the halfway plane is a disc of radius R.

The points of intersection of the molecular axes with the halfway plane (that is the centers of the molecules) define a two-dimensional lattice. When the molecules of the domain are vertically oriented we refer to this lattice as the *reference lattice* (see [4, figure 4]). In the case of vertically oriented molecules, the optimal packing of spherocylindrical (rod-like) molecules is *hexagonal*, and consequently the reference lattice has three principal and three secondary axes of symmetry [1]. The reference lattice is used to define the needed coordinate systems.

2.2. *Coordinate systems*

Using the symmetry axes of the reference lattice, we introduce three coordinate systems (see [4, figure 5]). The first is the $(\hat{x}, \hat{y}, \hat{z})$-coordinate system which is fixed to the halfway plane, and defined as follows: (i) the z-axis coincides with the axis of the circumscribing cylinder (the axis of the virtual domain), and as such it is normal to the interface; (ii) the intersection of the z-axis with the halfway plane defines the origin of coordinates; (iii) the xy-plane coincides with the halfway plane; (iv) the x-axis coincides with one of the secondary axes of symmetry; (v) the y-axis coincides with one of the principal axes of symmetry. Due to the hexagonal symmetry of the reference lattice, the above system of coordinates is orthogonal. As the molecules are tilted, the halfway plane moves relative to the interface and this $(\hat{x}, \hat{y}, \hat{z})$ coordinate system moves with it.

The $(\hat{m}, \hat{n}, \hat{z})$-coordinate system is also fixed to the halfway plane. It is obtained from the $(\hat{x}, \hat{y}, \hat{z})$-coordinate system by a rotation of angle ϕ about the $\hat{z}$-axis. Hence

$$\begin{pmatrix} \hat{m} \\ \hat{n} \end{pmatrix} = \begin{pmatrix} \cos\phi & \sin\phi \\ -\sin\phi & \cos\phi \end{pmatrix} \begin{pmatrix} \hat{i} \\ \hat{j} \end{pmatrix}, \tag{1}$$

where $\hat{i}$ and $\hat{j}$ are unite vectors along $\hat{x}$ and $\hat{y}$, respectively. Finally, the space fixed coordinate system $(\hat{X}, \hat{Y}, \hat{Z})$ is attached to the interface. Its origin is on the interface. Its $\hat{Z}$-axis is collinear with the $\hat{z}$-axis. Its $\hat{X}\hat{Y}$-plane coincides with the interface, and its

$\hat{X}$ and $\hat{Y}$ axes are parallel to $\hat{x}$ and $\hat{y}$, respectively. Hence the $(\hat{X}, \hat{Y}, \hat{Z})$ and $(\hat{x}, \hat{y}, \hat{z})$ coordinate systems are related by the vertical translation

$$\{\vec{X}, \vec{Y}, \vec{Z}\} = \left\{\vec{x}, \vec{y}, \left(z + r_0 + \frac{h}{2}\cos\theta\right)\hat{z}\right\}. \tag{2}$$

2.3. Tilting operator

The transition from the *reference lattice* of vertically aligned molecules, to the lattice of parallely aligned but arbitrarily oriented molecules is made by using the *tilting operator* $\mathbf{\Lambda}_{\hat{n}}(\theta)$ as given in [3]:

$$\mathbf{\Lambda}_{\hat{n}}(\theta) = \mathbf{T}_{\hat{n}}(\theta)\mathbf{O}_{\hat{n}}(\theta), \tag{3}$$

where $\mathbf{O}_{\hat{n}}(\theta)$ is the rotation operator by angle θ about the $\hat{n}$-axis, and is given by [75]:

$$\mathbf{O}_{\hat{n}}(\theta) = (\cos\theta)I + (\sin\theta)\hat{n}\times + (1 - \cos\theta)\hat{n}\hat{n}\bullet \tag{4}$$

and $\mathbf{T}_{\hat{n}}(\theta)$ is the *local realignment operator* given by [3]:

$$\mathbf{T}_{\hat{n}}(\theta) = I - (\tan\theta)\hat{n}\times. \tag{5}$$

Explicitly, the tilting operator $\mathbf{\Lambda}_{\hat{n}}(\theta)$ is given by [3]:

$$\mathbf{\Lambda}_{\hat{n}}(\theta) = (\sec\theta)I + (1 - \sec\theta)\hat{n}\hat{n}\bullet, \tag{6}$$

where the axis of tilting lies in the halfway plane, and is in the $\hat{n} = -\hat{i}\sin\phi + \hat{j}\cos\phi$ direction. The tilting angle, relative to the normal to the interface, is θ. The tilting of a molecule takes place in a plane passing through its center and parallel to the $\hat{m}\hat{z}$-plane where $\hat{m} = \hat{i}\cos\phi + \hat{j}\sin\phi$ and $\hat{z}$ is normal to the interface. The tilting operator can alternatively be written in terms of ϕ, as in [3]:

$$\begin{aligned}\mathbf{\Lambda}(\theta, \phi) = (\sec\theta)I + (1 - \sec\theta)& \\ \times \left[\left(\sin^2\phi\right)\hat{i}\hat{i} - (\sin\phi\cos\phi)\left(\hat{i}\,\hat{j} + \hat{j}\hat{i}\right) + \left(\cos^2\phi\right)\hat{j}\,\hat{j}\right]\bullet&.\end{aligned} \tag{7}$$

3. Lattice structure

The lattice of the centers of the molecules of the domain is the basic structure of molecular organization at the domain level. Consequently, it is important to have at our disposal a variety of different (but of course equivalent) mathematical expressions describing it. For close packed, parallely aligned and vertically oriented, spherocylindrical molecules, the lattice formed by the centers of the molecules is given, relative to the $(\hat{x}, \hat{y}, \hat{z})$-coordinate system, by [2]

$$\vec{r}_{\ell k} \equiv \vec{r}_{\ell k}(0, 0) = r_0\left[\hat{i}\sqrt{3}\ell + \hat{j}(2k - \ell)\right], \tag{8}$$

where ℓ and k are integers. The zeros in the argument of $r_{\ell k}$ indicate that the above lattice corresponds to the case $(\theta, \phi) = (0, 0)$, that is the case of vertically aligned molecules.

The lattice of arbitrarily oriented spherocylindrical molecules is obtained by applying the tilting operator, as given by equations (6) or (7), to $\vec{r}_{\ell k}(0,0)$:

$$\vec{r}_{\ell k}(\theta,\phi) = \mathbf{\Lambda}_{\hat{n}}(\theta)\vec{r}_{\ell k}(0,0) \equiv \mathbf{\Lambda}(\theta,\phi)\vec{r}_{\ell k}(0,0). \tag{9}$$

This is a compact form of the expression for the lattice of the centers of parallely aligned and arbitrarily oriented close packed spherocylindrical molecules at the liquid–gas interface.

It is worthwhile noting that equation (9) has a generality that goes beyond the case studied here (that is the case where $\vec{r}_{\ell k}(0,0)$ is the *reference lattice* for *hexagonally packed* molecules). Actually, equation (9) remains valid even when $\vec{r}_{\ell k}(0,0)$ is the *reference lattice* for *any type of packing*. What $\mathbf{\Lambda}_{\hat{n}}(\theta)$, or, equivalently, $\mathbf{\Lambda}(\theta,\phi)$, expresses mathematically is the transformation (as measured by an observer stationed in the halfway plane) undergone by a lattice site as the corresponding molecule tilts subject to the constraint that its polar head remains tangent to the interface, and its cylindrical part remains tangent to its neighbors.

3.1. Reference lattice

Let $\alpha_{\ell k}$ designate the *phase angle* of lattice site (ℓ, k), defined as the angle that the reference lattice radius vector $\vec{r}_{\ell k}(0,0)$ makes with the x-axis (the NNN direction). Then, due to equation (8), the phase angle $\alpha_{\ell k}$ is given by

$$\tan\alpha_{\ell k} = \frac{2k-\ell}{\sqrt{3}\ell}, \tag{10}$$

$$\cos\alpha_{\ell k} = \frac{\sqrt{3}\ell}{2\sqrt{k^2+\ell^2-k\ell}}, \tag{11}$$

$$\sin\alpha_{\ell k} = \frac{2k-\ell}{2\sqrt{k^2+\ell^2-k\ell}}. \tag{12}$$

Making use of equations (11) and (12), we can rewrite equation (8) as

$$\frac{\vec{r}_{\ell k}(0,0)}{2r_0\sqrt{k^2+\ell^2-k\ell}} = \hat{\imath}\cos\alpha_{\ell k} + \hat{\jmath}\sin\alpha_{\ell k} \tag{13}$$

and due to equation (A.12) (see appendix A), it reduces to:

$$\frac{\vec{r}_{\ell k}(0,0)}{2r_0\sqrt{k^2+\ell^2-k\ell}} = \mathbf{O}_{\hat{k}}(\alpha_{\ell k})\hat{\imath}. \tag{14}$$

Equation (13) expresses the reference lattice in the $(\hat{x},\hat{y},\hat{z})$ coordinate system, and equation (14) generates the reference lattice from a unit vector along the $\hat{x}$-axis. Alternatively, by making use of equations (A.2) and (A.13), we can generate the reference lattice from a unit vector along the $\hat{m}$-axis,

$$\frac{\vec{r}_{\ell k}(0,0)}{2r_0\sqrt{k^2+\ell^2-k\ell}} = \mathbf{O}_{\hat{k}}(\alpha_{\ell k}-\phi)\hat{m}(\phi) \tag{15}$$

and due to equation (A.12) it is expressed in the $(\hat{m}, \hat{n}, \hat{z})$-coordinate system as:

$$\frac{\vec{r}_{\ell k}(0,0)}{2r_0\sqrt{k^2+\ell^2-k\ell}} = \hat{m}(\phi)\cos(\alpha_{\ell k}-\phi) + \hat{n}(\phi)\sin(\alpha_{\ell k}-\phi). \tag{16}$$

3.2. Standard form

When the tilting operator, as given by equation (7), is applied to the reference lattice of hexagonally close packed molecules, as given by equation (8), the resulting explicit expression for the lattice is:

$$\begin{aligned}\vec{r}_{\ell k}(\theta,\phi) = {}& \hat{i}r_0\big\{\ell\sqrt{3}\big(\sin^2\phi + \sec\theta\cos^2\phi\big) + (2k-\ell)(\sec\theta-1)\sin\phi\cos\phi\big\} \\ & + \hat{j}r_0\big\{(2k-\ell)\big(\sec\theta\sin^2\phi+\cos^2\phi\big) + \ell\sqrt{3}(\sec\theta-1)\sin\phi\cos\phi\big\}.\end{aligned} \tag{17}$$

This is the first explicit expression for the lattice. It was derived in [3]. The length of the lattice radius vector is given by (see [4, equation (4)])

$$r_{\ell k}(\theta,\phi) = r_0\sqrt{4\big(\ell^2+k^2-k\ell\big) + \big[\sqrt{3}\ell\cos\phi + (2k-\ell)\sin\phi\big]^2\tan^2\theta}. \tag{18}$$

3.3. The function $u_{mn}(\theta,\phi)$

We define the function $u_{mn}(\theta,\phi)$ by

$$\begin{aligned}u_{mn}(\theta,\phi) = {}& \big(\sec^m\theta-1\big)\sin\phi\cos\phi \\ & + \frac{1}{2}\big[1+(-1)^m\big]\big[\sec^n\theta\sin^2\phi + \sec^{1-n}\theta\cos^2\phi\big].\end{aligned} \tag{19}$$

Equation (17) can then be rewritten in the form:

$$\begin{aligned}\vec{r}_{\ell k}(\theta,\phi) = {}& \hat{i}r_0\big\{\ell\sqrt{3}u_{00}(\theta,\phi) + (2k-\ell)u_{10}(\theta,\phi)\big\} \\ & + \hat{j}r_0\big\{(2k-\ell)u_{01}(\theta,\phi) + \ell\sqrt{3}u_{10}(\theta,\phi)\big\}.\end{aligned} \tag{20}$$

Making use of the Pythagorean identity, as well as the Ptolemy identities for the sine and cosine functions, respectively, the expression for $u_{mn}(\theta,\phi)$ can be rewritten as

$$\begin{aligned}2u_{mn}(\theta,\phi) = {}& \big(\sec^m\theta-1\big)\sin 2\phi \\ & + \frac{1}{2}\big[1+(-1)^m\big]\big[\big(\sec^{1-n}\theta+\sec^n\theta\big) + \big(\sec^{1-n}\theta-\sec^n\theta\big)\cos 2\phi\big].\end{aligned} \tag{21}$$

To evaluate (20) we need the expression of $u_{mn}(\theta,\phi)$ in the special cases $m = 0, 1$ and $n = 0, 1$. For $n = 0, 1$ the following trigonometric identity holds:

$$\sec^{1-n}\theta \pm \sec^n\theta = (\pm 1)^n(\sec\theta-1), \quad n = 0, 1. \tag{22}$$

Hence, for $n = 0, 1$, the expression for $u_{0n}(\theta,\phi)$ reduces to

$$u_{0n}(\theta,\phi) = \frac{1}{2}\big\{(\sec\theta+1) + (-1)^n(\sec\theta-1)\cos 2\phi\big\}, \quad n = 0, 1. \tag{23}$$

For $m = 1$, $u_{1n}(\theta, \phi)$ is independent of n and is easily seen to be given by

$$u_{1n}(\theta, \phi) = \frac{1}{2}(\sec\theta - 1)\sin 2\phi. \tag{24}$$

Substituting from equations (23) and (24), into (20), and grouping the coefficients of $(\sec\theta + 1)$ and $(\sec\theta - 1)$ in each component of $\vec{r}_{\ell k}(\theta, \phi)$, we obtain

$$\begin{aligned} 2\vec{r}_{\ell k}(\theta, \phi) = {} & \hat{i} r_0 \big\{ \ell\sqrt{3}(\sec\theta + 1) + (\sec\theta - 1)\big[(2k - \ell)\sin 2\phi + \ell\sqrt{3}\cos 2\phi\big]\big\} \\ & + \hat{j} r_0 \big\{ (2k - \ell)(\sec\theta + 1) \\ & \quad - (\sec\theta - 1)\big[(2k - \ell)\cos 2\phi - \ell\sqrt{3}\sin 2\phi\big]\big\}. \end{aligned} \tag{25}$$

This is the second explicit expression for the lattice of the centers of parallely aligned and arbitrarily oriented, hexagonally close packed spherocylindrical molecules. It underlines the Cartesian components of the lattice radius vector and brings out succinctly the functional dependence on the angles θ and ϕ.

3.4. The phase angle $\alpha_{\ell k}$

Making use of expressions (11) and (12) for $\cos\alpha_{\ell k}$ and $\sin\alpha_{\ell k}$, respectively, equation (25) can be rewritten as

$$\begin{aligned} & \frac{\vec{r}_{\ell k}(\theta, \phi)}{r_0\sqrt{k^2 + \ell^2 - k\ell}} \\ & \quad = \left\{ \begin{array}{l} \hat{i}[(\sec\theta + 1)\cos\alpha_{\ell k} + (\sec\theta - 1)(\cos\alpha_{\ell k}\cos 2\phi + \sin\alpha_{\ell k}\sin 2\phi)] \\ +\hat{j}[(\sec\theta + 1)\sin\alpha_{\ell k} - (\sec\theta - 1)(\sin\alpha_{\ell k}\cos 2\phi - \cos\alpha_{\ell k}\sin 2\phi)] \end{array} \right\} \end{aligned} \tag{26}$$

and using the Ptolemy trigonometric identities for the sum of two angles it reduces to

$$\frac{\vec{r}_{\ell k}(\theta, \phi)}{r_0\sqrt{k^2 + \ell^2 - k\ell}} = \left\{ \begin{array}{l} \hat{i}[(\sec\theta + 1)\cos\alpha_{\ell k} + (\sec\theta - 1)\cos(2\phi - \alpha_{\ell k})] \\ +\hat{j}[(\sec\theta + 1)\sin\alpha_{\ell k} + (\sec\theta - 1)\sin(2\phi - \alpha_{\ell k})] \end{array} \right\}. \tag{27}$$

This is the third explicit expression for the lattice of the centers of parallely aligned and arbitrarily oriented, hexagonally close packed spherocylindrical molecules. It underlines the Cartesian components of the lattice radius vector and brings out the role played by the phase angle $\alpha_{\ell k}$.

3.5. Decomposition of the lattice radius vector relative to the tilt azimuth ϕ

The radius vector $\vec{r}_{\ell k}(\theta, \phi)$ can be separated into two parts: one dependent on, and the other independent of, the tilt azimuth ϕ, leading to

$$\frac{\vec{r}_{\ell k}(\theta, \phi)}{r_0\sqrt{k^2 + \ell^2 - k\ell}} = \left\{ \begin{array}{l} (\sec\theta + 1)[\hat{i}\cos\alpha_{\ell k} + \hat{j}\sin\alpha_{\ell k}] \\ +(\sec\theta - 1)[\hat{i}\cos(2\phi - \alpha_{\ell k}) + \hat{j}\sin(2\phi - \alpha_{\ell k})] \end{array} \right\}. \tag{28}$$

By making use of equation (A.12), the above expression can be rewritten, in terms of the rotation operator, in the form:

$$\frac{\vec{r}_{\ell k}(\theta,\phi)}{r_0\sqrt{k^2+\ell^2-k\ell}} = \big[(\sec\theta+1)\mathbf{O}_{\hat{k}}(\alpha_{\ell k}) + (\sec\theta-1)\mathbf{O}_{\hat{k}}(2\phi-\alpha_{\ell k})\big]\hat{i}. \tag{29}$$

Making use of equation (14) for the *reference lattice* radius vector we obtain

$$\vec{r}_{\ell k}(\theta,\phi) = \frac{\sec\theta+1}{2}\vec{r}_{\ell k}(0,0) + (\sec\theta-1)r_0\sqrt{k^2+\ell^2-k\ell}\,\mathbf{O}_{\hat{k}}(-\alpha_{\ell k})\mathbf{O}_{\hat{k}}(2\phi)\hat{i}. \tag{30}$$

Equations (28)–(30) provide three variants of the fourth explicit form of the expression for the lattice of the centers of parallely aligned and arbitrarily oriented close packed spherocylindrical molecules. These expressions untangle and clearly underline the contributions of the three factors involved: θ (the tilting angle), ϕ (the tilt azimuth) and (ℓ, k), the generalized topological coordinates of the lattice site. The values of θ and (ℓ, k) influence both components of the vector $\vec{r}_{\ell k}(\theta,\phi)$, while ϕ only influences one of them.

3.6. *Decomposition of the lattice radius vector relative to the tilting angle θ*

Equation (29) for the lattice radius vector can be written as

$$\begin{aligned}\frac{\vec{r}_{\ell k}(\theta,\phi)}{r_0\sqrt{k^2+\ell^2-k\ell}} = \big\{(\sec\theta)\big[\mathbf{O}_{\hat{k}}(\alpha_{\ell k}) + \mathbf{O}_{\hat{k}}(2\phi-\alpha_{\ell k})\big] \\ + \big[\mathbf{O}_{\hat{k}}(\alpha_{\ell k}) - \mathbf{O}_{\hat{k}}(2\phi-\alpha_{\ell k})\big]\big\}\hat{i}\end{aligned} \tag{31}$$

and making use of identities (A.7) and (A.8) (see appendix A), it can be rewritten as

$$\frac{\vec{r}_{\ell k}(\theta,\phi)}{2r_0\sqrt{k^2+\ell^2-k\ell}} = \sec\theta\cos(\phi-\alpha_{\ell k})\hat{m}(\phi) - \sin(\phi-\alpha_{\ell k})\hat{n}(\phi). \tag{32}$$

Equation (31) can alternatively be written as

$$\frac{\vec{r}_{\ell k}(\theta,\phi)}{r_0\sqrt{k^2+\ell^2-k\ell}} = \big\{2\mathbf{O}_{\hat{k}}(\alpha_{\ell k}) + (\sec\theta-1)\big[\mathbf{O}_{\hat{k}}(\alpha_{\ell k}) + \mathbf{O}_{\hat{k}}(2\phi-\alpha_{\ell k})\big]\big\}\hat{i}. \tag{33}$$

By making use of equation (14) for the reference lattice, the above equation reduces to

$$\vec{r}_{\ell k}(\theta,\phi) = \vec{r}_{\ell k}(0,0) + (\sec\theta-1)r_0\sqrt{k^2+\ell^2-k\ell}\big[\mathbf{O}_{\hat{k}}(\alpha_{\ell k}) + \mathbf{O}_{\hat{k}}(2\phi-\alpha_{\ell k})\big]\hat{i} \tag{34}$$

and due to identity (A.8), it further reduces to the following form:

$$\vec{r}_{\ell k}(\theta,\phi) = \vec{r}_{\ell k}(0,0) + 2(\sec\theta-1)r_0\sqrt{k^2+\ell^2-k\ell}\cos(\phi-\alpha_{\ell k})\hat{m}(\phi). \tag{35}$$

Equations (31)–(35) underline the dependence of the lattice radius vector on the tilting angle θ. Equation (31) is in operator form, while equation (32) is in vector form relative to the $(\hat{m},\hat{n},\hat{z})$ coordinate system. Expressions (34) and (35) relate the lattice radius vector $\vec{r}_{\ell k}(\theta,\phi)$ to the reference lattice radius vector $\vec{r}_{\ell k}(0,0)$.

3.7. Lattice generating operator

We define the lattice generating operator $\mathbf{G}_{\ell k}(\theta, \phi)$, by

$$\vec{r}_{\ell k}(\theta, \phi) = r_0 \mathbf{G}_{\ell k}(\theta, \phi)\hat{i} \tag{36}$$

and, due to equations (29), (31) and (33), it is given by

$$\frac{\mathbf{G}_{\ell k}(\theta, \phi)}{\sqrt{k^2 + \ell^2 - k\ell}} = (\sec\theta + 1)\mathbf{O}_{\hat{k}}(\alpha_{\ell k}) + (\sec\theta - 1)\mathbf{O}_{\hat{k}}(2\phi - \alpha_{\ell k}) \tag{37}$$

or, equivalently, by

$$\frac{\mathbf{G}_{\ell k}(\theta, \phi)}{\sqrt{k^2 + \ell^2 - k\ell}} = \left\{ \begin{array}{l} (\sec\theta)[\mathbf{O}_{\hat{k}}(\alpha_{\ell k}) + \mathbf{O}_{\hat{k}}(2\phi - \alpha_{\ell k})] \\ +[\mathbf{O}_{\hat{k}}(\alpha_{\ell k}) - \mathbf{O}_{\hat{k}}(2\phi - \alpha_{\ell k})] \end{array} \right\} \tag{38}$$

or, equivalently, by

$$\frac{\mathbf{G}_{\ell k}(\theta, \phi)}{\sqrt{k^2 + \ell^2 - k\ell}} = 2\mathbf{O}_{\hat{k}}(\alpha_{\ell k}) + (\sec\theta - 1)\big[\mathbf{O}_{\hat{k}}(\alpha_{\ell k}) + \mathbf{O}_{\hat{k}}(2\phi - \alpha_{\ell k})\big]. \tag{39}$$

The operator $\mathbf{G}_{\ell k}(\theta, \phi)$ generates the whole lattice from a unite vector along the x-axis. Note that the x-axis is a secondary axis of symmetry of the reference lattice (it is in the NNN direction). As a test of correspondence, the special case $\phi = 0$ of the above expression for the lattice generating operator is worked out in appendix B, and it correctly generates the lattice obtained in [2] for this special case.

Equation (36) in conjunction with (37), (38) or (39), is the fifth form of the expression for the lattice of the centers of parallely aligned and arbitrarily oriented, close packed spherocylindrical molecules.

Both the tilting operator and the lattice generating operator, take advantage of the abstract form of the rotation operator as given in [75]. They both produce the lattice of the centers of the tilted molecules. The tilting operator generates the lattice of tilted molecules from the *reference lattice* as input, and is valid for any type of packing. The lattice generating operator generates the lattice of tilted molecules from the unite vector along the NNN *direction*, but its applicability is restricted to hexagonal packing.

4. Analysis

In this section we study the characteristics of the lattice, using the results obtained in section 3 above. We will be mainly concerned with symmetry (see [76]), loci (see [77]), envelops (see [78,79]) and stationary points. All of the analytical results obtained in this section can of course also be proved by projective geometrical arguments.

4.1. The symmetry

The lattice generating operator has C_2 (2-fold) symmetry with respect to the angle ϕ. That is,

$$\mathbf{G}_{\ell k}(\theta, \phi + \pi) = \mathbf{G}_{\ell k}(\theta, \phi). \tag{40}$$

Equation (40) has its physical origin in the C_2 symmetry of the spherocylindrical molecules, and is easily seen to follow from expression (37) due to the univaluedness of the rotation operator as a function of ϕ, that is, $\mathbf{O}_{\hat{k}}(\omega + 2\pi) = \mathbf{O}_{\hat{k}}(\omega)$.

4.2. The locus line

From equation (35) for the lattice radius vector it is seen that, as θ varies while holding ϕ, ℓ and k fixed, the locus of lattice site (ℓ, k) traces a straight line that we designate by $\vec{L}_{\ell k}(\theta, \phi)$. This locus line is in the $\hat{m}(\phi)$ direction, and is linear in $(\sec\theta - 1)$.

The tangent $\vec{T}^{(L)}_{\ell k}(\theta, \phi)$ to the locus line is equal to the partial derivative of $\vec{r}_{\ell k}(\theta, \phi)$ with respect to θ, and is given by

$$\vec{T}^{(L)}_{\ell k}(\theta, \phi) = \frac{\partial}{\partial\theta}\vec{r}_{\ell k}(\theta, \phi) = 2(\sec\theta\tan\theta)r_0\sqrt{k^2 + \ell^2 - k\ell}\cos(\phi - \alpha_{\ell k})\hat{m}(\phi). \tag{41}$$

As could have been anticipated from the physical considerations of the present problem, the tangent is in the $\hat{m}(\phi)$ direction for all values of θ and all lattice sites (ℓ, k). The speed $\vec{V}^{(L)}_{\ell k}(\theta, \phi)$ with which the lattice site moves along the locus line varies nonlinearly with θ according to $\sec\theta\tan\theta$; it varies sinusoidally with ϕ according to $\cos(\phi - \alpha_{\ell k})$; and it varies with the site coordinates ℓ and k according to $\sqrt{k^2 + \ell^2 - k\ell}$.

4.3. The locus circle

As ϕ varies from 0 to π, the vector $\mathbf{O}_{\hat{k}}(2\phi)\hat{i}$ rotates through a complete circle. Consequently, from equation (30) for the lattice radius vector it can easily be seen that, as ϕ varies while holding θ, ℓ and k fixed, the locus of lattice site (ℓ, k) traces a circle that we designate by $C_{\ell k}(\theta)$. This locus circle has a radius given by

$$a_{\ell k}(\theta) = (\sec\theta - 1)r_0\sqrt{k^2 + \ell^2 - k\ell} \tag{42}$$

and it is centered at

$$\vec{c}_{\ell k}(\theta) = \left(\frac{\sec\theta + 1}{2}\right)\vec{r}_{\ell k}(0, 0). \tag{43}$$

As expected, for $\theta = 0$, the locus circle $C_{\ell k}(\theta)$ collapses to a point (as seen from equation (42)), located at $\vec{r}_{\ell k}(0, 0)$ (as seen from equation (43)).

In terms of the parameters of the locus circle, the lattice radius vector takes the form:

$$\vec{r}_{\ell k}(\theta, \phi) = \vec{c}_{\ell k}(\theta) + a_{\ell k}(\theta)\mathbf{O}_k(2\phi - \alpha_{\ell k})\hat{i}. \tag{44}$$

As ϕ varies from 0 to π, while holding θ, ℓ and k fixed, the tip of the lattice radius vector $\vec{r}_{\ell k}(\theta,\phi)$ scans the points on the circumference of the locus circle $C_{\ell k}(\theta)$. The radius $a_{\ell k}(\theta)$ of the locus circle increases with θ according to $(\sec\theta - 1)$ and it increases with the site coordinates ℓ, k according to $\sqrt{k^2+\ell^2-k\ell}$. The radius vector $\vec{c}_{\ell k}(\theta)$ from the origin to the center of the locus circle increases with θ according to $(\sec\theta + 1)$.

The tangent $\vec{T}^{(C)}_{\ell k}(\theta,\phi)$ to the locus circle is equal to the partial derivative of $\vec{r}_{\ell k}(\theta,\phi)$ with respect to ϕ, and is given by

$$\vec{T}^{(C)}_{\ell k}(\theta,\phi) = \frac{\partial}{\partial\phi}\vec{r}_{\ell k}(\theta,\phi) = 2(\sec\theta - 1)r_0\sqrt{k^2+\ell^2-k\ell}\,\mathbf{O}_k(2\phi-\alpha_{\ell k})\hat{k}\times\hat{i}, \quad (45)$$

where we have made use of equation (A.11), for the derivative of the rotation operator.

4.4. *Common point of tangency*

Theorem 1. The point $P_{\ell k}$ at lattice site (ℓ, k) of the reference lattice $\vec{r}_{\ell k}(0,0)$ is a common point of tangency for all the locus circles $C_{\ell k}(\theta)$.

Proof. Let the angle $\phi_{\ell k}$ be defined by

$$\phi_{\ell k} = \frac{\pi}{2} + \alpha_{\ell k} \quad (46)$$

and note that

$$\cos(\phi_{\ell k} - \alpha_{\ell k}) = 0, \qquad \mathbf{O}_k(2\phi_{\ell k} - \alpha_{\ell k}) = \mathbf{O}_k(\alpha_{\ell k})\mathbf{O}_k(\pi). \quad (47)$$

Evaluating equation (35) at $\phi = \phi_{\ell k}$ we obtain

$$\vec{r}_{\ell k}(\theta,\phi)\big|_{\phi=\phi_{\ell k}} = \vec{r}_{\ell k}(0,0). \quad (48)$$

From equations (44), (45) and (48) it is seen that:

(i) $P_{\ell k}$ is a common point on all the locus circles $C_{\ell k}(\theta)$.

(ii) As the lattice site (ℓ, k) moves on the locus circle $C_{\ell k}(\theta)$, it reaches point $P_{\ell k}$ at $\phi = \phi_{\ell k}$ irrespective of the value of θ.

(iii) The *direction* of the tangent vector $\vec{T}^{(C)}_{\ell k}(\theta,\phi)$ to locus circle $C_{\ell k}(\theta)$ does not depend on the value of θ.

Hence the *direction* of the tangent vector $\vec{T}^{(C)}_{\ell k}(\theta,\phi)$ evaluated at $P_{\ell k}$ is the same for all the locus circles $C_{\ell k}(\theta)$. This implies that all the locus circles $C_{\ell k}(\theta)$ are tangent to each other at $P_{\ell k}$, and this completes the proof of theorem 1. □

Evaluating equation (45) at $\phi = \phi_{\ell k}$ we obtain the expression for the tangent vector at the common point of tangency $P_{\ell k}$ as

$$\vec{T}^{(C)}_{\ell k}(\theta,\phi)\big|_{\phi=\phi_{\ell k}} = -2(\sec\theta - 1)r_0\sqrt{k^2+\ell^2-k\ell}\,\mathbf{O}_k(\alpha_{\ell k})\hat{k}\times\hat{i}. \quad (49)$$

The above equation can also be written as

$$\vec{T}^{(C)}_{\ell k}(\theta,\phi)\big|_{\phi=\phi_{\ell k}} = -(\sec\theta - 1)\hat{k} \times \vec{r}_{\ell k}(0,0), \tag{50}$$

that is the tangent vector $\vec{T}^{(C)}_{\ell k}(\theta,\phi)$ is perpendicular to $\vec{r}_{\ell k}(0,0)$ at $P_{\ell k}$.

Theorem 2. The common point of tangency $P_{\ell k}$ is the point nearest to the origin on the circumference of the locus circle $C_{\ell k}(\theta)$ for all values of the tilting angle θ.

Proof. Since the physically allowed range of values of the tilting angle θ is $0 \leqslant \theta \leqslant \pi/2$, then in this range $\sec\theta \pm 1 \geqslant 0$. Given this fact, it can then be seen from equation (29) that $\vec{r}_{\ell k}(\theta,\phi)$ is made up of the sum of two vectors who's lengths are $r_0\sqrt{k^2+\ell^2-k\ell}(\sec\theta+1) \geqslant 0$ and $r_0\sqrt{k^2+\ell^2-k\ell}(\sec\theta-1) \geqslant 0$, respectively, and who's directions are $\mathbf{O}_{\hat{k}}(\alpha_{\ell k})\hat{i}$ and $\mathbf{O}_{\hat{k}}(2\phi-\alpha_{\ell k})\hat{i}$, respectively. Due to equation (47), for $\phi = \phi_{\ell k}$, the directions of these two vectors become $\mathbf{O}_{\hat{k}}(\alpha_{\ell k})\hat{i}$ and $\mathbf{O}_{\hat{k}}(\pi+\alpha_{\ell k})\hat{i}$, respectively. That is, for $\phi = \phi_{\ell k} = \pi/2 + \alpha_{\ell k}$, the two vectors making up $\vec{r}_{\ell k}(\theta,\phi)$ are antiparallel and, consequently, the length of the radius vector $\vec{r}_{\ell k}(\theta,\phi)$ is minimum for this value of ϕ.

But for $\phi = \phi_{\ell k}$, $\vec{r}_{\ell k}(\theta,\phi) = \vec{r}_{\ell k}(0,0)$ and the tip of $\vec{r}_{\ell k}(0,0)$ coincides with $P_{\ell k}$. Furthermore, according to theorem 1, $P_{\ell k}$ is the common point of tangency. Hence the common point of tangency $P_{\ell k}$, of the locus circles $C_{\ell k}(\theta)$ associated with lattice site (ℓ, k), is the point nearest to the origin on the circumference of the locus circle $C_{\ell k}(\theta)$ for all values of the tilting angle θ. This completes the proof of theorem 2. □

4.5. The stationary point

As the tilt azimuth ϕ varies (holding θ and ℓ, k fixed), the lattice sites do vary as described by equation (30). That is, the points of intersection of the molecular axes with the half-way plane do vary with ϕ. Nevertheless, in this section we will demonstrate that (i) the projection (on the half-way plane) of the molecular axis does have a stationary point which is independent of the direction of inclination ϕ, (ii) that this stationary point is also independent of the inclination angle θ, and, finally, (iii) that this double stationary point coincides with the common point of tangency $P_{\ell k}$.

4.5.1. Projection of the molecular axis

The vector $\overrightarrow{c_0c_q}$ joining the *center of the molecule* to the projection (on the halfway plane) of the *center of the molecular hemisphere no.* q, where $q = 1, 2$ (see [4, figure 7]), is given (via [4, equation (6)]), by

$$\overrightarrow{c_0c_q} = (-1)^q\left(\frac{h\sin\theta}{2}\right)\hat{m}(\phi), \quad q = 1, 2. \tag{51}$$

Since the radius vector from the origin to the center of the molecule is given by $\vec{r}_{\ell k}(\theta, \phi)$, then the *parametric equation* of the *projection* (on the halfway plane) of the *axis of the molecule* centered at lattice site (ℓ, k) is given by:

$$\vec{\lambda}_{\ell k}(\theta, \phi, \beta) = \vec{r}_{\ell k}(\theta, \phi) + \beta r_0 \sqrt{k^2 + \ell^2 - k\ell}\hat{m}(\phi),$$
$$|\beta| \leqslant \left(\frac{h \sin\theta + 2r_0}{2r_0\sqrt{k^2 + \ell^2 - k\ell}} \right). \tag{52}$$

Making use of equation (32) for $\vec{r}_{\ell k}(\theta, \phi)$, and extending the projection indefinitely in both directions, the above equation can be rewritten as

$$\frac{\vec{\lambda}_{\ell k}(\theta, \phi, \beta)}{r_0\sqrt{k^2 + \ell^2 - k\ell}} = \big[\beta + \sec\theta \cos(\phi - \alpha_{\ell k})\big]\hat{m}(\phi) - \sin(\phi - \alpha_{\ell k})\hat{n}(\phi), \tag{53}$$

where β is now a dimensionless variable in the range $-\infty \leqslant \beta \leqslant +\infty$.

4.5.2. Variation of the projection with ϕ

The variation with ϕ of the points along the projection of the molecular axis on the halfway plane can be obtained from equation (53) by making use of equation (A.15) (see appendix A). This leads to

$$\frac{\partial}{\partial\phi}\left(\frac{\vec{\lambda}_{\ell k}(\theta, \phi, \beta)}{r_0\sqrt{k^2 + \ell^2 - k\ell}} \right) = \left\{ \begin{array}{l} [\partial\beta/\partial\phi - (\sec\theta - 1)\sin(\phi - \alpha_{\ell k})]\hat{m}(\phi) \\ +[\beta + (\sec\theta - 1)\cos(\phi - \alpha_{\ell k})]\hat{n}(\phi) \end{array} \right\}. \tag{54}$$

4.5.3. Existence of a stationary point

Let us assume for a moment that a *stationary point*, with respect to ϕ, on the projection of the molecular axis, does exist. Let the parameter β at this stationary point be given by the function $\beta_{\ell k}(\theta, \phi)$. Let the radius vector from the origin to this stationary point be denoted by $\vec{\lambda}_{\ell k}$. That is

$$\vec{\lambda}_{\ell k} = \vec{\lambda}_{\ell k}(\theta, \phi, \beta)\big|_{\beta = \beta_{\ell k}(\theta, \phi)}, \tag{55}$$

where we have already anticipated, in the choice of notation, that the stationary point will be independent, not only of ϕ, but also of θ. The condition for the existence of the stationary point is

$$\left.\frac{\partial\vec{\lambda}_{\ell k}(\theta, \phi, \beta)}{\partial\phi}\right|_{\beta = \beta_{\ell k}(\theta, \phi)} = 0 \tag{56}$$

and it is easily seen from equation (54) that the above condition (56) has a solution given by

$$\beta_{\ell k}(\theta, \phi) = -(\sec\theta - 1)\cos(\phi - \alpha_{\ell k}). \tag{57}$$

4.5.4. Radius vector of the stationary point

Combining equations (53), (55) and (57), leads to the following expression for the radius-vector from the origin to the stationary point on the projection of the molecular axis:

$$\frac{\vec{\lambda}_{\ell k}}{r_0\sqrt{k^2+\ell^2-k\ell}} = \hat{m}(\phi)\cos(\phi-\alpha_{\ell k}) - \hat{n}(\phi)\sin(\phi-\alpha_{\ell k}). \tag{58}$$

This stationary point is, by construction, independent of ϕ, and as seen from equation (58) it is also independent of θ. By comparing equations (16) and (58) we find that

$$\vec{\lambda}_{\ell k} = \vec{r}_{\ell k}(0,0), \tag{59}$$

that is the stationary point coincides with the common point of tangency $P_{\ell k}$. The above results can be stated as

Theorem 3. The common point of tangency $P_{\ell k}$, (which is also site (ℓ, k) of the reference lattice), is the double stationary point (with respect to θ and ϕ) of the projection (on the half-way plane) of the molecular axis passing through lattice site (ℓ, k).

4.6. The envelope circle

As ϕ and θ vary, the projection of the molecular axis, as parametrized by equations (52) and (53), has a stationary point $\vec{\lambda}_{\ell k} = \vec{r}_{\ell k}(0,0)$ given by equation (59). Consequently, the projection, as a function of ϕ and θ, of the cylindrical part of the molecule, forms a family of curves with ϕ and θ as variable parameters. This family of curves has as envelope, a circle of radius r_0, centered at $\vec{\lambda}_{\ell k} = \vec{r}_{\ell k}(0,0)$. In this section we will give an analytic proof of this statement.

4.6.1. Projection of the molecular cylinder

Since the projection of the molecular axis on the half-way plane is in the $\hat{m}(\phi)$ direction (as can be seen from equation (51)), and since $\vec{\lambda}_{\ell k}(\theta,\phi,\beta)$ provides a parametric representation of the radius vector from the origin to the different points on this projection of the molecular axis on the half-way plan, then the parametric representation of the radius vector $\vec{\kappa}^{\pm}_{\ell k}(\theta,\phi,\beta)$, from the origin to points on the two boundaries of the projection of the *molecular cylinder* on the half-way plane (see [4, figure 7]), is given by

$$\vec{\kappa}^{\pm}_{\ell k}(\theta,\phi,\beta) = \vec{\lambda}_{\ell k}(\beta,\theta,\phi) \pm r_0\hat{n}(\phi). \tag{60}$$

Making use of equations (52) and (53) for $\vec{\lambda}_{\ell k}(\theta,\phi,\beta)$, the above parametric equation for $\vec{\kappa}^{\pm}_{\ell k}(\theta,\phi,\beta)$ can be rewritten in the following alternative forms:

$$\begin{aligned}\vec{\kappa}^{\pm}_{\ell k}(\theta,\phi,\beta) &= \vec{r}_{\ell k}(\theta,\phi) + \beta r_0\sqrt{k^2+\ell^2-k\ell}\,\hat{m}(\phi) \pm r_0\hat{n}(\phi),\\ |\beta| &\leqslant \left(\frac{h\sin\theta}{2r_0\sqrt{k^2+\ell^2-k\ell}}\right)\end{aligned} \tag{61}$$

or

$$\frac{\vec{\kappa}^{\pm}_{\ell k}(\theta,\phi,\beta)}{r_0\sqrt{k^2+\ell^2-k\ell}} = \big[\beta + \sec\theta\cos(\phi-\alpha_{\ell k})\big]\hat{m}(\phi) - \left[\sin(\phi-\alpha_{\ell k}) \mp \frac{1}{\sqrt{k^2+\ell^2-k\ell}}\right]\hat{n}(\phi). \tag{62}$$

4.6.2. The two special points on the projection of the molecular cylinder

Corresponding to $\beta = \beta_{\ell k}(\theta,\phi)$, as given by equation (57), there are two special points on the boundary of the projection of the cylindrical part of the molecule. Their radius vectors from the origin are given by:

$$\vec{\kappa}^{\pm}_{\ell k}(\theta,\phi,\beta)\big|_{\beta=\beta_{\ell k}(\theta,\phi)} = \vec{\lambda}_{\ell k}(\theta,\phi,\beta)\big|_{\beta=\beta_{\ell k}(\theta,\phi)} \pm r_0\hat{n}(\phi) \tag{63}$$

and due to equations (55) and (59) the above equation reduces to

$$\vec{\kappa}^{\pm}_{\ell k}(\theta,\phi,\beta)\big|_{\beta=\beta_{\ell k}(\theta,\phi)} = \vec{r}_{\ell k}(0,0) \pm r_0\hat{n}(\phi). \tag{64}$$

We denote these special points by $\vec{K}^{\pm}_{\ell k}(\phi)$,

$$\vec{K}^{\pm}_{\ell k}(\phi) = \vec{\kappa}^{\pm}_{\ell k}(\theta,\phi,\beta)\big|_{\beta=\beta_{\ell k}(\theta,\phi)} \tag{65}$$

and due to equation (64), as well as equation (A.14) (see appendix A), they are given by

$$\vec{K}^{\pm}_{\ell k}(\phi) = \vec{r}_{\ell k}(0,0) \pm r_0 O_{\hat{k}}(\phi)\hat{j}. \tag{66}$$

4.6.3. The envelope circle of the family of projections

Equation (66) clearly shows that, as the variable parameter ϕ varies from 0 to 2π, each branch of $\vec{K}^{\pm}_{\ell k}(\phi)$ traces a circle centered at $\vec{r}_{\ell k}(0,0)$ and having r_0 as radius. This is expressed by the following theorem.

Theorem 4. The common point of tangency $P_{\ell k}$, (which is also site (ℓ,k) of the reference lattice), is the center of the envelope circle for the family of lines (with angles ϕ and θ as variable parameters) forming the boundaries of the projection (on the half-way plane) of the cylindrical part of the molecule centered at lattice site (ℓ,k).

5. Graphical representations

5.1. Global lattice

5.1.1. Variation with θ

Figure 1 shows the variation of the lattice sites with the tilting angle θ for fixed tilt azimuth ϕ. The tilting angle θ varies from 0° to 80° degrees in steps of 5° degrees. The values of the tilt azimuth are $\phi = 0°, 60°, 90°$ and $-45°$ for figures 1(a)–(d), respectively.

As expected from equation (35), the loci of the lattice sites are straight lines in the $\hat{m}$-direction (the direction of ϕ) with angle θ as variable parameter. One can see that the

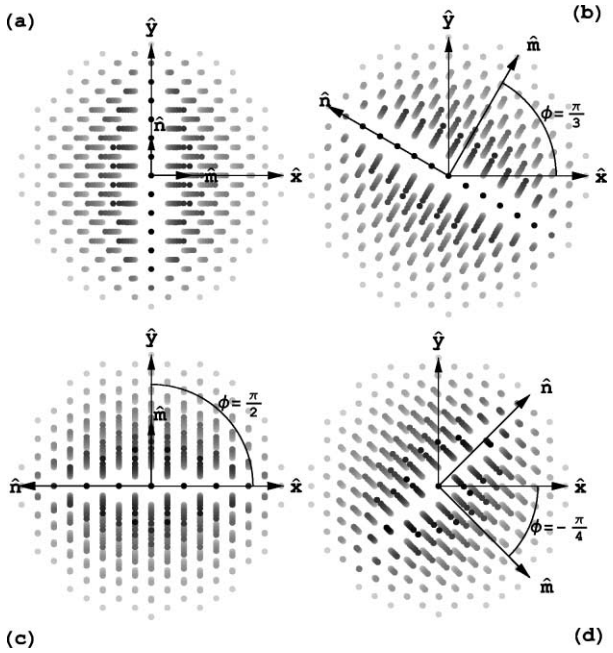

Figure 1. Variation of the lattice sites with the tilting angle θ for fixed tilt azimuth ϕ. The angle θ varies from 0° to 80° in steps of 5°. (a) $\phi = 0^\circ$, (b) $\phi = 60^\circ$, (c) $\phi = 90^\circ$, (d) $\phi = -45^\circ$.

rate at which the lattice site moves along the locus line accelerates with θ. This is consistent with the predicted speed which is proportional to $\sec\theta \tan\theta$ (see equation (41)). From this same equation it is also seen that this speed has a $\sqrt{k^2 + \ell^2 - k\ell}$ dependence on the generalized coordinates (ℓ, k), and so the speed of the lattice site along the locus line should increases as we go further out from the origin. This feature is also born out by the graphic simulations of figures 1(a)–(d).

For $\phi = 0^\circ$, 60° and 90°, the $\hat{n}$-axis (which is the tilting axis) coincides with one of the axes of symmetry of the references lattice, and there are reference lattice sites situated along it. As the molecules of the domain are tilted, the centers of these molecules should remain stationary, and this feature is also born out by the graphic simulations. For $\phi = -45^\circ$, there are no reference lattice sites on the tilting axis $\hat{n}$, except the site at the origin. Hence there is only one stationary site (i.e., only one locus which is a point) in this case.

The boldness of the lattice sites in figure 1 is directly proportional to the value of the tilt angle θ. Note that, as we approach the boundaries, the locus lines get truncated at increasingly lower tilt angles. That is, as we approach the boundaries, the surviving sites (centers of molecules that are fully bounded by the domain) correspond to increasingly lower tilt. The boundaries of the domain are determined by the procedure developed in [4], using a domain diameter R given by $R/r_0 = 15$ and molecules having a cylindrical length h given by $h/r_0 = 20$. r_0 is the radius of the molecular cylinder, and it sets the length scale.

5.1.2. Variation with ϕ

Figure 2 shows the variation of the lattice sites with the tilt azimuth ϕ for fixed tilt angle θ. The angle ϕ varies from 0° to 180° in steps of 10°. The values of the tilting angle θ are $\theta = 30°, 45°, 60°$ and 75° for figures 2(a), (b), (c) and (d), respectively.

The loci of all lattice sites are circles, as expected from equation (44). A variation of π degrees in ϕ takes the lattice sites through a complete cycle due to the C_2 symmetry of the problem. The radius of the locus circles increases as we go further out from the origin. This is due to its $\sqrt{k^2 + \ell^2 - k\ell}$ dependence on the generalized coordinates (ℓ, k), as seen from equation (42). Furthermore, as the inclination angle θ increases (in going from figures 2(a)–(d)), the radii of the corresponding locus circles also increase due to the $(\sec\theta - 1)$ factor of equation (42). Consequently, due to these combined effects, the overlapping of the locus circles takes place for increasingly smaller values of (ℓ, k), as the value of the tilt angle θ increases.

The boldness of the lattice sites is directly proportional to the value of the tilt azimuth ϕ. Note that, as we approach the boundaries, the locus circles get truncated. The boundaries are determined by the procedure developed in [4], using a domain diameter R given by $R/r_0 = 15$ and molecules having a cylindrical length h given by $h/r_0 = 20$, where r_0 is the radius of the molecular cylinder.

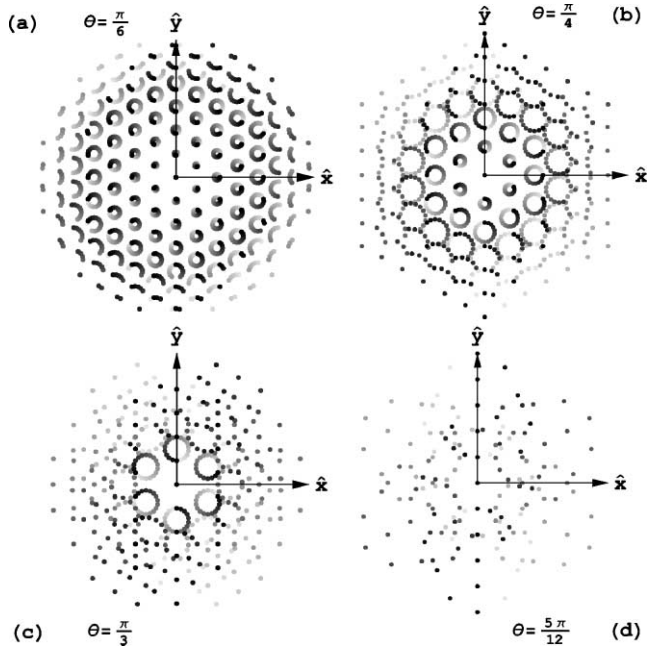

Figure 2. Variation of the lattice sites with the tilt azimuth ϕ for fixed tilt angle θ. The angle ϕ varies from 0° to 180° degrees in steps of 10°. (a) $\theta = 30°$; (b) $\theta = 45°$; (c) $\theta = 60°$; (d) $\theta = 75°$.

5.2. One lattice site

5.2.1. Variation with θ

Figure 3 shows the variation of lattice site (ℓ, k) with the tilt angle θ for fixed values of tilt azimuth ϕ. The angle θ varies from 0° to 60° in steps of 10°. In figure 3(a), $\phi = 0°$ and $(\ell, k) = (1, 3)$. In figure 3(b), $\phi = -30°$ and $(\ell, k) = (2, 3)$. In figure 3(c), $\phi = 45°$ and $(\ell, k) = (3, 3)$. In figure 3(d), $\phi = 60°$ and $(\ell, k) = (4, 3)$. The length h of the cylindrical part of the molecule is given by $h/r_0 = 8$, where r_0 is the radius of the molecular cylinder.

The locus of the lattice site is a straight line in the $\hat{m}$ direction (see equation (35)), and the $\sec\theta \tan\theta$ factor in the speed of the lattice site along the locus line (see equation (41)) is (at least qualitatively) visible.

5.2.2. Variation with ϕ

Figures 4–6 show the variation of a lattice site (ℓ, k) with the tilt azimuth ϕ for fixed tilt angle θ. The tilt azimuth ϕ varies from 0° to 180°. For all of three figures the values of θ in the subfigures are given by (a) $\theta = 30°$; (b) $\theta = 45°$; (c) $\theta = 60°$; and (d) $\theta = 75°$. The length h of the cylindrical part of the molecule is given by $h/r_0 = 8$, where r_0 is the radius of the molecular cylinder. Since the radius of the envelop circle is constant (it is equal to the molecular radius r_0), it can serve as a comparative reference scale for the subfigures.

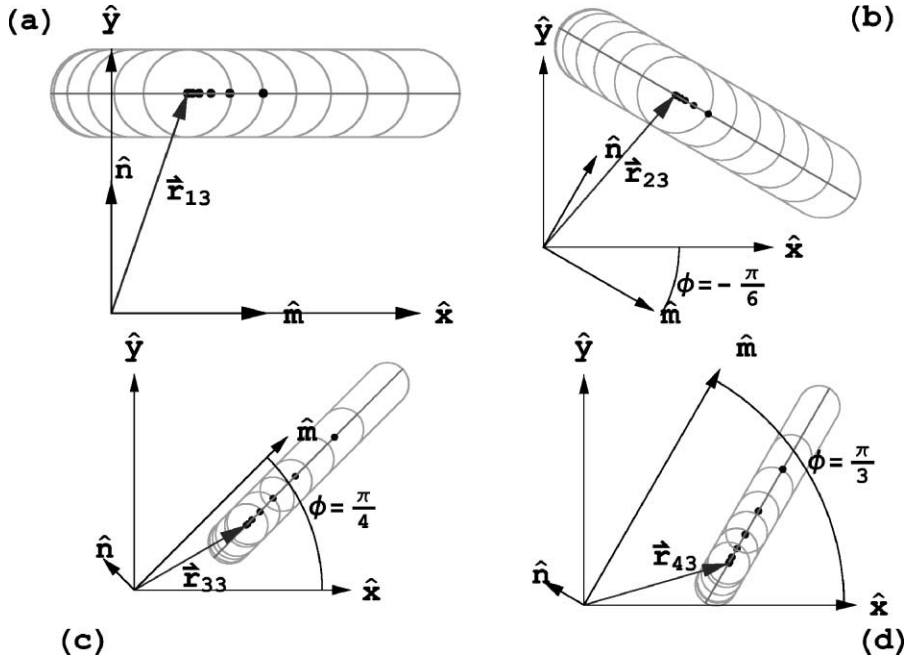

Figure 3. Variation of lattice site $(\ell, k) = (1, 3)$ with the tilt angle θ for a tilt azimuth $\phi = 0°$. The angle θ varies from 0° to 60° in steps of 10°.

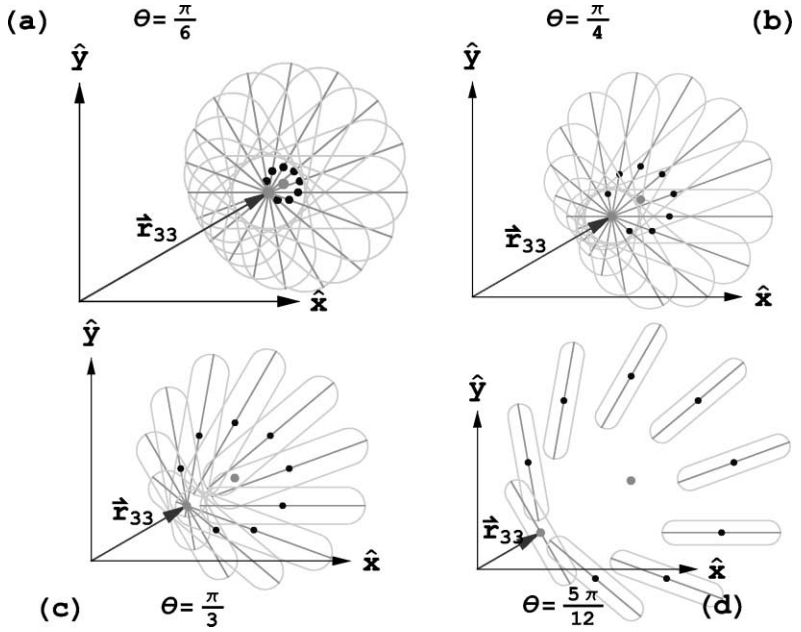

Figure 4. The variation of lattice site $(\ell, k) = (3, 3)$ with the tilt azimuth ϕ. ϕ varies from 0° to 180° by steps of 20°. (a) $\theta = 30°$; (b) $\theta = 45°$; (c) $\theta = 60°$; (d) $\theta = 75°$.

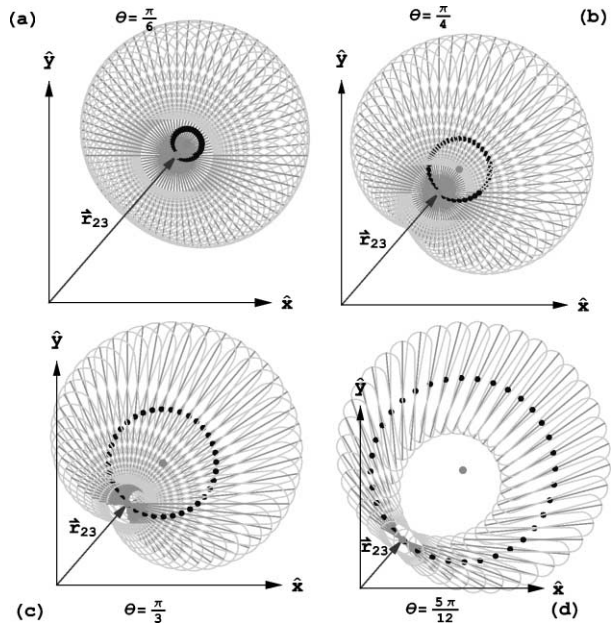

Figure 5. The variation of lattice site $(\ell, k) = (2, 3)$ with the tilt azimuth ϕ for fixed tilt angle θ. The azimuth ϕ varies from 0° to 180° by small steps of 5°.

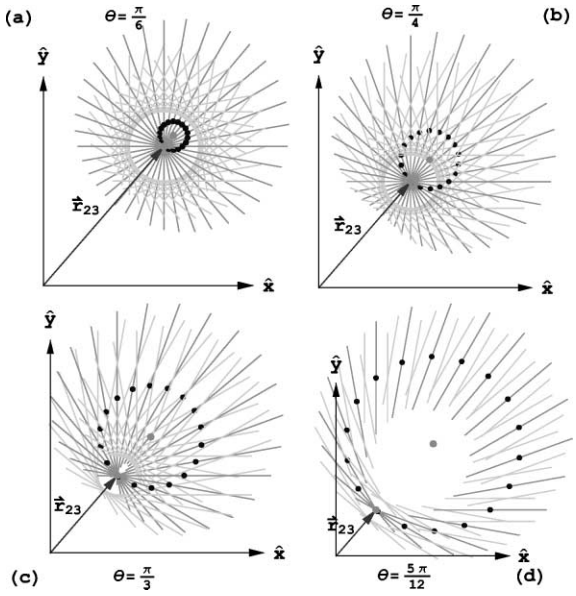

Figure 6. The variation of lattice site $(\ell, k) = (2, 3)$ with the tilt azimuth ϕ for tilt angle $\theta = 60°$. The azimuth ϕ varies from 0° to 180° by steps of 10°.

We note that:

(i) The locus of the lattice site is a circle (see equation (44)).

(ii) The center of this locus circle lies on the prolongation of the radius vector $\vec{r}_{\ell k} \equiv \vec{r}_{\ell k}(0, 0)$ (see equation (43)).

(iii) This locus circle passes through point $P_{\ell k}$ having $\vec{r}_{\ell k} \equiv \vec{r}_{\ell k}(0, 0)$ as radius vector (see theorem 1).

(iv) $P_{\ell k}$ is the point on the locus circle which is nearest to the origin (see theorem 2).

(v) The projections of the molecular axis on the plane of the lattice (the half-way plane), all intersect at $P_{\ell k}$ (see theorem 3).

(vi) This point of intersection $P_{\ell k}$ is the center of the envelope circle for the boundaries of the projections of the molecular cylinder (see theorem 4).

In figure 4, (ℓ, k) is set to $(3, 3)$, and the tilt azimuth ϕ is varied in large steps of $\Delta\phi = 20°$ in order to clearly bring out the details listed above.

In figure 5, (ℓ, k) is set to $(2, 3)$ and the tilt azimuth ϕ is varied in small steps of $\Delta\phi = 5°$ in order to bring out the global characteristics of the variation of the lattice point with ϕ.

In figure 6, (ℓ, k) is set to $(2, 3)$ (as in figure 5), but the tilt azimuth ϕ is varied in intermediate steps of $\Delta\phi = 10°$ in order to simultaneously bring out the detailed as well as the global characteristics of the variation of the lattice point with ϕ. Furthermore, the

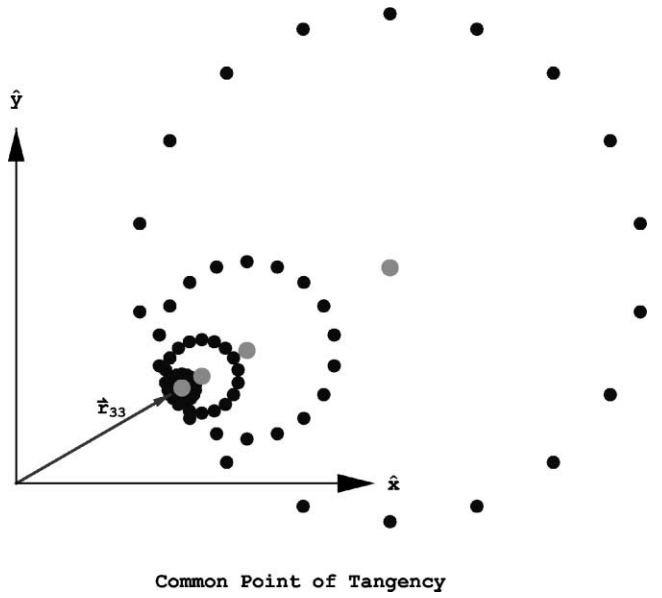

Figure 7. The variation of lattice site $(\ell, k) = (3, 3)$ with the tilt azimuth ϕ and the tilt angle θ. ϕ varies from 0° to 180° in steps of 10°, while θ varies from 30° to 75° in steps of 15°. Also shown are the centers of the locus circles.

molecular hemispheres have been suppressed in order to better identify the characteristics listed above, specially for large values of the tilt angle θ where the figures become visually rather complicated.

5.2.3. Combined variation with θ and ϕ

In the previous figures we studied separately, and in detail, the variation of the lattice sites with the tilting angle θ and with the azimuth angle ϕ. In figures 7–10 we will study the combined effect of θ and ϕ on a lattice site. In all four figures, (ℓ, k) is set equal to (3, 3), ϕ varies from 0° to 180° in steps of 10°, and θ varies from 30° to 75° in steps of 15°. Figure 7 shows the loci of the lattice site and the centers of the locus circles. Figure 8 shows the loci of the projection of the molecular axis. Figure 9 shows the loci of the boundary of the molecular projection. Figure 10 shows the loci of the full molecular projection.

6. Conclusion

This paper is the fifth in a series of articles [1–4] that progressively and systematically develop a detailed analytical molecular model for Langmuir films. The main results of the present paper are:

(i) The introduction (via equations (25), (27), (29), (30)–(33) and (35)) of several *new expressions* for the lattice radius vector.

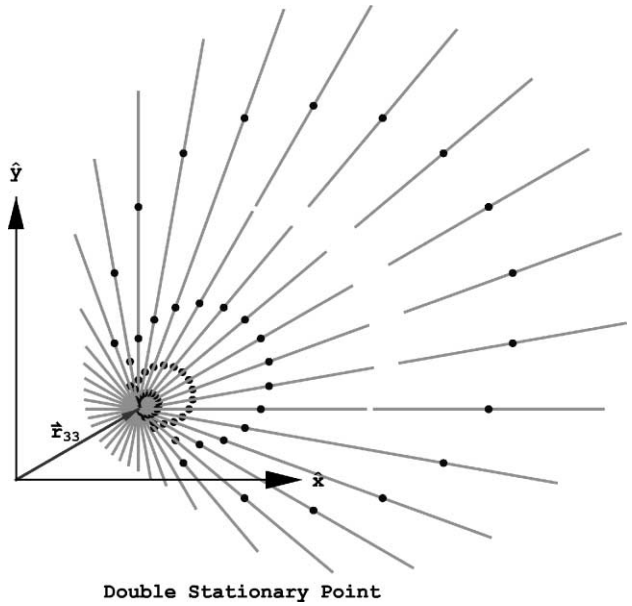

Figure 8. The variation of lattice site $(\ell, k) = (3, 3)$, as well as the projection of the molecular axis, with the tilt azimuth ϕ and the tilt angle θ. ϕ varies from 0° to 180° in increments of 10°, while θ varies from 30° to 75° in increments of 15°. Also shown are the centers of the locus circles.

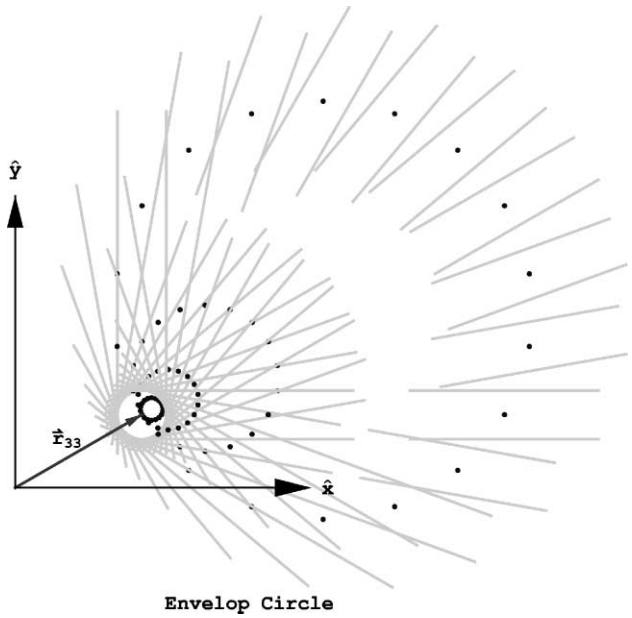

Figure 9. The variation of lattice site $(\ell, k) = (3, 3)$, as well as the boundaries of the molecular projection, with the tilt azimuth ϕ and tilt angle θ. ϕ varies from 0° to 180° in increments of 10°, while θ varies from 30° to 75° in increments of 15°.

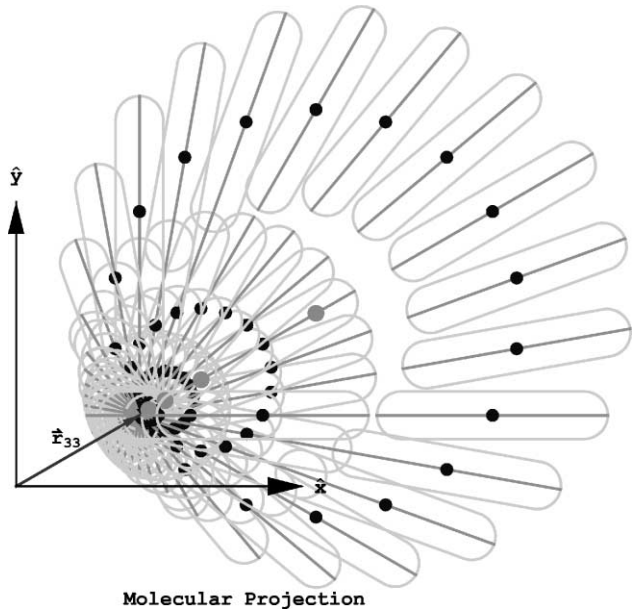

Figure 10. The variation of lattice site $(\ell, k) = (3, 3)$, as well as the molecular projection, with the tilt azimuth ϕ and tilt angle θ. ϕ varies from 0° to 180° in steps of 10°, while θ varies from 30° to 75° in steps of 15°. Also shown are the centers of the locus circles.

(ii) The introduction (via equation (10)) of the *phase angle* $\alpha_{\ell k}$ associated with a lattice site.

(iii) The introduction (via equations (37)–(39)) of the *lattice generating operator* $\mathbf{G}_{\ell k}(\theta, \phi)$.

(iv) The proof that the *locus* of a lattice site (as the angle ϕ goes through a complete cycle) is a circle.

(v) The determination (via equations (42) and (43)) of the *parameters* of this locus circle.

(vi) The proof (via theorem 1) of the existence of a *common point of tangency* for the locus circles corresponding to different values of the tilting angle θ.

(vii) The proof (via theorem 1) that the common points of tangency coincide with the sites of the reference lattice.

(viii) The proof (via theorem 2) of a *minimality* characteristic of the common point of tangency.

(ix) The proof (via theorem 3) of the existence of a *double stationary point* on the projection (on the half-way plane) of the molecular axis.

(x) The proof (via theorem 3) that this stationary point coincides with the common point of tangency.

(xi) The proof (via theorem 4) that the envelope of the family of lines (with angle ϕ as a variable parameter) forming the boundaries of the projection (on the half-way plane) of the cylindrical part of the molecule is a circle.

(xii) The determination (via equation (66)) of the parameters of this envelope circle.

(xiii) The proof (via theorem 4 and equation (66)) that the center of this envelope circle lies at the common point of tangency.

The importance of the above results resides in the fact that domains are the building blocks of Langmuir films, and that the lattice formed by the centers of their molecules is the backbone of their molecular organization.

Acknowledgements

The present work was supported by a research grant from the Natural Sciences and Engineering Research Council of Canada (NSERC). It is a pleasure to acknowledge the help of Michel Piché in obtaining hard copies of the articles cited in the bibliography. The programming language Mathematica version 3.0.1.1x [80], was used to produce the high resolution graphics presented in the paper. The computations were performed on a 500 MHz Apple Macintosh G4 computer with 1 Gigabit of live memory and 27 Gigabits of hard disk space.

Appendix A. Rotation operator

This appendix is essentially a compendium of expressions related to the rotation operator and used in the main text of the paper. The operator for a finite rotation by angle $\pm\omega$ about an axis $\hat{q}$ is given, via equation (4), by

$$\mathbf{O}_{\hat{q}}(\pm\omega) = (\cos\omega)I \pm (\sin\omega)\hat{q}\times + (1-\cos\omega)\hat{q}\hat{q}\bullet . \tag{A.1}$$

Successive rotations about the same axis are associative and commutative:

$$\mathbf{O}_{\hat{q}}(\alpha+\beta) = \mathbf{O}_{\hat{q}}(\alpha)\mathbf{O}_{\hat{q}}(\beta) = \mathbf{O}_{\hat{q}}(\beta)\mathbf{O}_{\hat{q}}(\alpha). \tag{A.2}$$

A.1. Operator identities

From equation (A.1) we have

$$\begin{aligned}\mathbf{O}_{\hat{q}}(\omega) \pm \mathbf{O}_{\hat{q}}(-\omega) = (1\pm 1)(\cos\omega)I + (1\mp 1)(\sin\omega)\hat{q}\times \\ + (1\pm 1)(1-\cos\omega)\hat{q}\hat{q}\bullet .\end{aligned} \tag{A.3}$$

For a vector $\vec{\rho}$ which is perpendicular to the $\hat{q}$ axis, $\hat{q}\bullet\vec{\rho} = 0$ and, identity (A.3) leads to the following two very useful identities

$$\left[\mathbf{O}_{\hat{q}}(\omega) + \mathbf{O}_{\hat{q}}(-\omega)\right]\vec{\rho} = 2(\cos\omega)\vec{\rho} \tag{A.4}$$

and

$$\left[\mathbf{O}_{\hat{q}}(\omega) - \mathbf{O}_{\hat{q}}(-\omega)\right]\vec{\rho} = 2(\sin\omega)\hat{q} \times \vec{\rho}. \tag{A.5}$$

Identities (A.4) and (A.5) could have as easily been proved by simple geometrical arguments applied to the parallelogram rule of vector addition. On the other hand, the operator formalism provides a concise language for stating the mathematical arguments and relations.

As an application of these identities we will evaluate an expression that arises in the main part of the paper. Making use of identity (A.2), and the fact that $\mathbf{O}_{\hat{k}}(-\phi)\mathbf{O}_{\hat{k}}(\phi) = I$ we have

$$\left[\mathbf{O}_{\hat{k}}(\alpha_{\ell k}) \pm \mathbf{O}_{\hat{k}}(2\phi - \alpha_{\ell k})\right]\hat{i} = \left[\mathbf{O}_{\hat{k}}(\alpha_{\ell k} - \phi) \pm \mathbf{O}_{\hat{k}}(\phi - \alpha_{\ell k})\right]\mathbf{O}_{\hat{k}}(\phi)\hat{i} \tag{A.6}$$

and due to identities (A.4) and (A.5), and the fact that $\mathbf{O}_{\hat{k}}(\phi)\hat{i} = \hat{m}(\phi)$, we have the two relations:

$$\left[\mathbf{O}_{\hat{k}}(\alpha_{\ell k}) + \mathbf{O}_{\hat{k}}(2\phi - \alpha_{\ell k})\right]\hat{i} = 2\cos(\phi - \alpha_{\ell k})\hat{m}(\phi) \tag{A.7}$$

and

$$\left[\mathbf{O}_{\hat{k}}(\alpha_{\ell k}) - \mathbf{O}_{\hat{k}}(2\phi - \alpha_{\ell k})\right]\hat{i} = -2\sin(\phi - \alpha_{\ell k})\hat{n}(\phi). \tag{A.8}$$

A.2. Operator derivative

The derivative of the operator $\mathbf{O}_{\hat{q}}(\omega)$ is given by

$$\frac{\partial}{\partial\omega}\mathbf{O}_{\hat{q}}(\omega) = \lim_{\delta\omega\to 0}\frac{\mathbf{O}_{\hat{q}}(\omega+\delta\omega) - \mathbf{O}_{\hat{q}}(\omega)}{\delta\omega} = \mathbf{O}_{\hat{q}}(\omega)\lim_{\delta\omega\to 0}\frac{\mathbf{O}_{\hat{q}}(\delta\omega) - I}{\delta\omega} \tag{A.9}$$

and since (see [75]) as seen from equation (A.1)

$$\mathbf{O}_{\hat{q}}(\delta\omega) = I + (\delta\omega)\hat{q}\times \tag{A.10}$$

then, combining equations (A.9) and (A.10) we have

$$\frac{\partial}{\partial\omega}\mathbf{O}_{\hat{q}}(\omega) = \mathbf{O}_{\hat{q}}(\omega)\hat{q}\times \tag{A.11}$$

which is the desired result.

A.3. Special cases

For a vector $\vec{\rho}$ which is perpendicular to the $\hat{q}$ axis, $\hat{q}\bullet\vec{\rho} = 0$ and expression (A.1) leads to

$$\mathbf{O}_{\hat{q}}(\omega)\vec{\rho} = (\cos\omega)\vec{\rho} + (\sin\omega)\hat{q} \times \vec{\rho}. \tag{A.12}$$

Due to the definition of the $(\hat{m}, \hat{n}, \hat{z})$ coordinate system, we have

$$\hat{m}(\phi) = \mathbf{O}_{\hat{k}}(\phi)\hat{i} = \hat{i}\cos\phi + \hat{j}\sin\phi, \tag{A.13}$$

$$\hat{n}(\phi) = \mathbf{O}_{\hat{k}}(\phi)\hat{j} = \hat{j}\cos\phi - \hat{i}\sin\phi \tag{A.14}$$

and making use of equation (A.11) for the derivative of the rotation operator, and the fact that $\hat{k} \times \hat{m}(\phi) = \hat{n}(\phi)$ and $\hat{k} \times \hat{n}(\phi) = -\hat{m}(\phi)$, leads to

$$\frac{\partial \hat{m}(\phi)}{\partial \phi} = \hat{n}(\phi), \qquad \frac{\partial \hat{n}(\phi)}{\partial \phi} = -\hat{m}(\phi). \tag{A.15}$$

Combining identity (A.2) and equations (A.12)–(A.14), leads to:

$$\mathbf{O}_{\hat{k}}(2\phi - \alpha_{\ell k})\hat{i} = \hat{m}(\phi)\cos(\phi - \alpha_{\ell k}) + \hat{n}(\phi)\sin(\phi - \alpha_{\ell k}) \tag{A.16}$$

and

$$\mathbf{O}_{\hat{k}}(2\phi - \alpha_{\ell k})\hat{j} = \hat{n}(\phi)\cos(\phi - \alpha_{\ell k}) - \hat{m}(\phi)\sin(\phi - \alpha_{\ell k}). \tag{A.17}$$

Appendix B. Lattice generating operator for zero tilt azimuth

For $\phi = 0$, expression (38) for the Lattice Generating Operator $\mathbf{G}_{\ell k}(\theta, \phi)$ reduces to

$$\frac{\mathbf{G}_{\ell k}(\theta, 0)}{\sqrt{k^2 + \ell^2 - k\ell}} = (\sec\theta)\big[\mathbf{O}_{\hat{k}}(\alpha_{\ell k}) + \mathbf{O}_{\hat{k}}(-\alpha_{\ell k})\big] + \big[\mathbf{O}_{\hat{k}}(\alpha_{\ell k}) - \mathbf{O}_{\hat{k}}(-\alpha_{\ell k})\big] \tag{B.1}$$

and the lattice radius vector for $\phi = 0$ is given, via equation (36), by

$$\vec{r}_{\ell k}(\theta, 0) = r_0 \mathbf{G}_{\ell k}(\theta, 0)\hat{i}. \tag{B.2}$$

Combining equations (B.1) and (B.2) we have

$$\frac{\vec{r}_{\ell k}(\theta, 0)}{r_0\sqrt{k^2 + \ell^2 - k\ell}} = (\sec\theta)\big[\mathbf{O}_{\hat{k}}(\alpha_{\ell k}) + \mathbf{O}_{\hat{k}}(-\alpha_{\ell k})\big]\hat{i} + \big[\mathbf{O}_{\hat{k}}(\alpha_{\ell k}) - \mathbf{O}_{\hat{k}}(-\alpha_{\ell k})\big]\hat{i} \tag{B.3}$$

and making use of identities (A.4) and (A.5) of appendix Appendix A, the above expression for the lattice radius vector reduces to

$$\frac{\vec{r}_{\ell k}(\theta, 0)}{2r_0\sqrt{k^2 + \ell^2 - k\ell}} = \hat{i}\sec\theta\cos\alpha_{\ell k} + \hat{j}\sin\alpha_{\ell k} \tag{B.4}$$

and due to equations (11) and (12), it reduces further to

$$\vec{r}_{\ell k}(\theta, 0) = r_0\big[\big(\sqrt{3}\ell\sec\theta\big)\hat{i} + (2k - \ell)\hat{j}\big] \tag{B.5}$$

which is the result obtained in [3].

References

[1] J.-J. Max, A.F. Antippa and C. Chapados, Boundary effects in the hexagonal packing of rod-like molecules inside a right circular cylindrical domain I. The case of right circular spherocylindrical molecules, J. Math. Chem. 21 (1997) 339–358.

[2] A.F. Antippa, J.-J. Max and C. Chapados, Boundary effects in the hexagonal packing of rod-like molecules inside a right circular cylindrical domain II. The case of inclined spherocylindrical molecules, J. Math. Chem. 24 (1998) 79–108.

[3] A.F. Antippa, Tilting operator for phospholipidic molecular domains at the liquid–gas interface, J. Math. Chem. 26 (1999) 179–196.
[4] A.F. Antippa, J.-J. Max and C. Chapados, Boundary effects in the hexagonal packing of rod-like molecules inside a right circular cylindrical domain III. The case of arbitrarily oriented spherocylindrical molecules, J. Math. Chem. 30 (2001) 31–67.
[5] J.F. Nagle and S. Tristram-Nagle, Structure and interactions of lipid bilayers: role of fluctuations, in: *Lipid Bilayers*, eds. J. Katsaras and T. Gutberlet (Springer, Berlin, 2001) pp. 1–23.
[6] D. den Engelsen and B. de Koning, Ellipsometric study of organic monolayers. Part 1. Condensed monolayers, J. Chem. Soc. Farad. Trans. I 70 (1974) 1603–1614.
[7] M. Banville and A. Caill, Anisotropic molecules forming a monomolecular layer on a strongly adhesive substrate: a scaled particle treatment, Can. J. Phys. 61 (1983) 1592–1598.
[8] H.M. McConnell, Structures and transitions in lipid monolayers at the air–water interface, Ann. Rev. Phys. Chem. 42 (1991) 171–195.
[9] A. Ulman, *An Introduction to Ultrathin Organic Films from Langmuir–Blodgett to Self-Assembly* (Academic Press, Boston, 1991).
[10] J.A. Zasadzinski, R. Viswanathan, D.K. Schwartz, J. Garnaes, L. Madsen, S. Chiruvolu, J.T. Woodward and M.L. Longo, Applications of atomic force microscopy to structural characterization of organic thin films, Colloids and Surfaces A 93 (1994) 305–333.
[11] J.A. Zasadzinski, R. Viswanathan, L. Madsen, J. Garnaes and D.K. Schwartz, Langmuir–Blodgett films, Science 263 (1994) 1726–1733.
[12] J. Katsaras, X-ray diffraction studies of oriented lipid bilayers, Biochem. Cell Biol. 73 (1995) 209–218.
[13] C.M. Knobler, Phase behavior, ordering and self-assembly in monolayers, Physica A 236 (1997) 11–18.
[14] C.M. Knobler, The shapes of domains in two-phase monolayer systems, Nuovo Cimento D 20 (1998) 2095–2105.
[15] J. Katsaras and T. Gutberlet, *Lipid Bilayers* (Springer, Berlin, 2001).
[16] P. Dutta, J.B. Peng, B. Lin, J.B. Ketterson, M. Prakash, P. Georgopoulos and S. Ehrlich, X-ray diffraction studies of organic monolayers on the surface of water, Phys. Rev. Lett. 58 (1987) 2228–2231.
[17] K. Kjaer, J. Als-Nielsen, C.A. Helm, P. Tippman-Krayer and H. Mhwald, Synchrotron X-ray diffraction and reflection studies of arachidic acid monolayers at the air–water interface, J. Phys. Chem. 93 (1989) 3200–3206.
[18] J. Katsaras, K.R. Jeffrey, D.S-C. Yang and R.M. Epand, Direct evidence for the partial dehydration of phosphatidylethanolamine bilayers on approaching the hexagonal phase, Biochemistry 32 (1993) 10700–10707.
[19] J. Katsaras, R.H. Stinson and J.H. Davis, X-ray diffraction studies of oriented dilauroyl phosphatidylcholine bilayers in the L_δ and L_α phases, Acta Crystallographica B 50 (1994) 208–216.
[20] J. Katsaras, V.A. Raghunathan, E.J. Dufourc and J. Dufourcq, Evidence for a two-dimensional molecular lattice in subgel phase DPPC bilayers, Biochemistry 34 (1995) 4684–4688.
[21] J. Katsaras and V.A. Raghunathan, Molecular chirality and the ripple phase of phosphatidylcholine multibilayers, Phys. Rev. Lett. 74 (1995) 2022–2025.
[22] J. Katsaras, Structure of the subgel ($L_{c'}$) and gel ($L_{\beta'}$) phases of oriented dipalmitoylphosphatidylcholine multibilayers, J. Phys. Chem. 99 (1995) 4141–4147.
[23] R. Steitz, J.P. Peng, I.R. Peterson, I.R. Gentle, R.M. Kenn, M. Goldmann and G.T. Barnes, A grazing-incidence X-ray diffraction study of octadeconol monolayers at high surface pressures, Langmuir 14 (1998) 7245–7249.
[24] T.L. Kuhl, J. Maiewski, P.B. Howes, K. Kjaer, A. von Nahmen, K.Y.C. Lee, B. Ocko, J.N. Israelachvili and G.S. Smith, Packing stress relaxation in polymer-lipid monolayers at the air–water interface: An X-ray grazing-incidence diffraction and reflectivity study, J. Am. Chem. Soc. 121 (1999) 7682–7688.
[25] E. Teer, C.M. Knobler, A. Braslau, J. Daillant, C. Blot, D. Luzet, M. Goldmann and P. Fontiane, Transition between two next-nearest-neighbor phases in a mixed Langmuir monolayer. A study by

grazing incidence X-ray diffraction and Brewster-angle microscopy, J. Chem. Phys. 113 (2000) 2846–2850.

[26] E. Teer, C.M. Knobler, S. Siegel, D. Vollhardt and G. Brezesinski, Grazing incidence diffraction and Brewster-angle microscopy studies of mixtures of hexadecanoic acid and methyl hexadecanoate: The unexpected appearance of a phase with nearest-neighbor tilt, J. Phys. Chem. B 104 (2000) 10053–10058.

[27] C. Gourier, M. Alba, A. Braslau, J. Daillant, M. Goldmann, C.M. Knobler, F. Rieuford and G. Zalczer, Structure and elastic properties of 10–12 pentacosadiyonic acid Langmuir films, Langmuir 17 (2001) 6496–6505.

[28] D.K. Schwartz, J. Garnaes, R. Viswanathan and J.A.N. Zasadzinski, Surface order and stability of Langmuir–Blodgett films, Science 257 (1992) 508–511.

[29] X.-M. Yang, D. Xiao, S.-J. Xiao, Z.-H. Lu and Y. Wei, Observation of chiral domain morphology in a phospholipid Langmuir–Blodgett monolayer by atomic force microscopy, Phys. Lett. A 193 (1994) 195–198.

[30] X.-M. Yang, D. Xiao, S.-J. Xiao and Y. Wei, Domain structures of phospholipid monolayer Langmuir–Blodgett films determined by atomic force microscopy, Appl. Phys. A 59 (1994) 139–143.

[31] R. Viswanathan, J.A. Zasadzinski and D.K. Schwartz, Spontaneous chiral symmetry breaking by achiral molecules in a Langmuir–Blodgett film, Nature 368 (1994) 440–443.

[32] R. Viswanathan, L.L. Madsen, J.A. Zasadzinski and D.K. Schwartz, Liquid to hexatic to crystalline order in Langmuir–Blodgett films, Science 269 (1995) 51–53.

[33] S.-J. Xiao, H.-M. Wu, X.-M. Yang, Y. Wei, Z.-H. Tai and X.-Z. Sun, Atomic force microscopy studies of domain structures in phase-separated monolayers, Phys. Lett. A 193 (1994) 289–292.

[34] S.W. Hui, R. Viswanathan, J.A. Zasadzinski and J.N. Israelachvili, The structure and stability of phospholipid bilayers by atomic force microscopy, Biophys. J. 68 (1995) 171–178.

[35] H.-M. Wu, S.-J. Xiao, Z.-H. Tai and Y. Wei, Polymorphism of domains in phase-separated Langmuir–Blodgett films, Phys. Lett. A 199 (1995) 119–122.

[36] H.D. Sikes and D.K. Schwartz, Two-dimensional melting of an anisotropic crystal observed at the molecular level, Science 278 (1997) 1604–1606.

[37] J. Fang, M. Dennin, C.M. Knobler, Y. K. Godovsky, N.N. Makarova and H. Yokoyama, Structures of collapsed polysiloxane monolayers investigated by scanning force microscopy, J. Phys. Chem. B 101 (1997) 3147–3154.

[38] J. Fang, E. Teer, C.M. Knobler, K.-K. Loh and J. Rudnick, Boojums and shapes of domains in monolayer films, Phys. Rev. E 56 (1997) 1859–1868.

[39] K. Hisada and C.M. Knobler, Friction anisotropy and asymmetry related to the molecular tilt azimuth in a monolayer of 1-monopalmytoyl-rac-glycerol, Langmuir 16 (2000) 9390–9395.

[40] U. Gehlert, J. Fang and C.M. Knobler, Relating the organization of the molecular tilt azimuth to the lateral-force images in monolayers transferred to solid substrates, J. Phys. Chem. B 102 (1998) 2614–2617.

[41] T. Moenke-Wedler, G. Förster, G. Brezesinski, R. Steitz and I.R. Peterson, Diol monolayer structure on the water surface and on solid substrates, Langmuir 9, (1993) 2133–2140.

[42] B. Fischer, M.-W. Tsao, J. Ruiz-Gracia, T.M. Fischer, D.K. Schwartz and C.M. Knobler, Observation of a change from splay to bend orientation at a phase transition in a Langmuir monolayer, J. Phys. Chem. 98 (1994) 7430–7435.

[43] D.K. Schwartz, M.-W. Tsao and C.M. Knobler, Domain morphology in a two-dimensional anisotropic mesophase: Cups and boojum textures in a Langmuir monolayer, J. Chem. Phys. 101 (1994) 8258–8261.

[44] S. Rivière, S. Hénon, J. Meunier, D.K. Schwartz, M.-W. Tsao and C.M. Knobler, Texture and phase transitions in Langmuir monolayers of fatty acids. A comparative Brewster angle microscope and polarized fluorescence microscope study, J. Chem. Phys. 101 (1994) 10045–10051.

[45] M.-W. Tsao, T.M. Fischer and C.M. Knobler, Quantitative analysis of Brewster-angle microscopie images of tilt order in Langmuir monolayer domains, Langmuir 11 (1995) 3184–3188.
[46] M.N.G. de Mul and J.A. Mann, Jr., Determination of the thickness and optical properties of a Langmuir film from the domain morphology by Brewster angle microscopy, Langmuir 14 (1998) 2455–2466.
[47] J. Miñones, Jr., C. Carrera, P. Dynarowicz-Latka, J. Miñones, O. Conde, R. Seoane and J.M.R. Patino, Orientational changes of amphotericin B in Langmuir monolayers observed by Brewster angle microscopy, Langmuir 17 (2001) 1477–1482.
[48] J. Ignés-Mullol and D.K. Schwartz, Shear-induced molecular precession in a hexatic Langmuir monolayer, Nature 410 (2001) 348–351.
[49] H.M. McConnell, L.K. Tamm and R. Weis, Periodic structure in lipid monolayer phase transitions, Proc. Nat. Acad. Sci. USA (1984) 3249–3253.
[50] D.K. Schwartz and C.M. Knobler, Direct observation of transitions between condensed Langmuir monolayer phases by polarized fluorescence microscopy, J. Phys. Chem. 97 (1993) 8849–8851.
[51] D.K. Schwartz, J. Ruiz-Garcia, X. Qiu, J.V. Selinger and C.M. Knobler, Tilt stripe textures in Langmuir monolayers of fatty acids, Physica A 204 (1994) 606–615.
[52] C.M. Knobler, Ordering in two dimensions: Optical textures in monolayers, Nuovo Cimento D 16 (1994) 1367–1372.
[53] C. de la Riva, C. Kryschi and H.P. Trommsdorff, Optical spectroscopic study of the domain structure of triclinic p-terphenyl, Chem. Phys. Lett. 227 (1994) 13–18.
[54] K.J. Stine, S.A. Whitt and J.Y.-J. Uang, Fluorescence microscopy study of Langmuir monolayers of racemic and enantiomeric N-stearoyltyrosine, Chemistry and Physics of Lipids 69 (1994) 41–50.
[55] J.H. van Each, R.J.M. Nolte, H. Ringsdorf and G. Wildburg, Monolayers of chiral imidazole amphiphiles: Domain formation and metal complexation, Langmuir 10 (1994) 1955–1961.
[56] D.P. Parazak, J.Y.-J. Uang, S.A. Whitt and K.J. Stine, Fluorescence microscopy observations of domain structures in Langmuir monolayers of N-stearoylserine methyl ester and N-stearoylvaline at intermediate enantiomeric compositions, Chemistry and Physics of Lipids 75 (1995) 155–161.
[57] B. Fischer, M.-W. Tsao, J. Ruiz-Gracia, Th.M. Fischer, D.K. Schwartz and C.M. Knobler, The Blooming transition in Langmuir monolayers and its microscopic origin, Thin Solid Films 284–285 (1996) 110–114.
[58] J. Fang, U. Gehlert, R. Shashidar and C.M. Knobler, Imaging the azimuthal tilt order in monolayers by liquid crystal optical amplification, Langmuir 15 (1999) 297–299.
[59] J. Katsaras, Highly aligned lipid membrane systems in the physiologically relevant "excess water" condition, Biophys. J. 73 (1997) 2924–2929.
[60] J. Katsaras, Alignable biomimetic membranes, Physica B 241–243 (1998) 1178–1180.
[61] G. Pabst, J. Katsaras and V.A. Raghunathan, Enhancement of steric repulsion with temperature in oriented lipid multilayers, Phys. Rev. Lett. 88 (2002) 128101-1–128101-4.
[62] K. Hisada and C.M. Knobler, Microscopic friction anisotropy and asymmetry related to the molecular tilt azimuth in a monolayer of glycerol ester, Colloids and Surfaces A 198–200 (2002) 21–30.
[63] Y. Lyatskaya, Y. Liu, S. Tristram-Nagle, J. Katsaras and J.F. Nagle, Method for obtaining structure and interactions from oriented lipid bilayers, Phys. Rev. E 63 (2000) 11907-1–11907-9.
[64] C.M. Knobler, Langmuir monolayers and liquid crystals, Mol. Cryst. and Liq. Cryst. 364 (2001) 133–140.
[65] A.J. Kox, J.P.J. Michels and F.W. Wiegel, Simulation of a lipid monolayer using molecular dynamics, Nature 287 (1980) 317–319.
[66] S. Toxvaerd, Molecular dynamics simulation of domain formation in Langmuir monolayers of molecules with dipole moments, Mol. Phys. 95 (1998) 539–547.
[67] B.A. Pethica, M.L. Glasser and J. Mingins, Intermolecular forces in monolayers and air/water interfaces, J. Colloid. Interface Sci. 81 (1981) 41–51.

[68] V.M. Kaganer, M.A. Osipov and I.R. Peterson, A molecular model for tilting phase transitions between condensed phases of Langmuir monolayers, J. Chem. Phys. 98 (1993) 3512–3527.
[69] J. Israelachvili, Self-assembly in two dimensions: Surface micelles and domain formation in monolayers, Langmuir 10 (1994) 3774–3781.
[70] T.M. Fischer, R.F. Bruinsma and C.M. Knobler, Textures of surfactant monolayers, Phys. Rev. E 50 (1994) 413–428.
[71] A. Firouzi, D. Kumar, L.M. Bull, T. Besier, P. Sieger, Q. Huo, S.A. Walker, J.A. Zasadzinski, C. Glinka, J. Nicol, D. Margolese, G.D. Stucky and B.F. Chmelka, Cooperative organization of inorganic-surfactant and biomimetic assemblies, Science 267 (1995) 1138–1143.
[72] H.A. Stone and H.M. McConnell, Lipid domain instabilities in monolayers overlying sublayers of finite depth, J. Phys. Chem. 99 (1995) 13505–13508.
[73] H.A. Stone and H.M. McConnell, Hydrodynamics of quantized shape transitions of lipid domains, Proc. Roy. Soc. London Ser. A 448 (1995) 97–112.
[74] D. Duque and E. Chacon, Aggregation models at high packing fraction, Phys. Rev. E 62 (2000) 7147.
[75] A.F. Antippa, On the derivation of the rotation operator, Can. J. Phys. 75 (1997) 581–589.
[76] M. Tinkham, *Group Theory and Quantum Mechanics* (McGraw-Hill, New York, 1964) p. 53.
[77] L.P. Eisenhart, *Coordinate Geometry* (Ginn and Company, 1939) pp. 20–25.
[78] C. Zwikker, *The Advanced Geometry of Plane Curves and Their Applications* (Dover, New York, 1963) pp. 176–185.
[79] W.A. Granville, P.F. Smith and W.R. Longley, *Elements of the Differential and Integral Calculus* (Blaisdell, Waltham, MA, 1957) pp. 466–469.
[80] S. Wolfram, *Mathematica* (Cambridge University Press, Cambridge, MA, 1996).